Extraction of Building Footprints from Different Unmanned Aerial Vehicle (UAV) Platforms

Nabila Ismail, Khairul Nizam Tahar*

Centre of Studies for Surveying Science and Geomatics, Faculty of Architecture, Planning and Surveying,
Universiti Teknologi MARA, 40450 Shah Alam, Selangor Darul Ehsan, Malaysia.
*Corresponding author E-mail: khairul0127@salam.utim.edu.my

Abstract

The demand for map updating is increasing especially for developing countries. Therefore, rapid data acquisition of an urban area is needed. This study proposes unmanned platform as one of the solutions for rapid data acquisition to update the map for developing countries. The objective of this study is to perform the extraction of building footprints using fixed-wing unmanned aerial vehicle (UAV) and multi-rotor UAV. All images acquired from both UAVs were processed using different image matching algorithms to perform relative orientation. The building footprints were extracted based on different orthophoto results. The building footprints were evaluated in terms of area and length. The results show the area based matching method records the accurate result in term of area and length assessment which are about 13m^2 and 1.4m respectively. The results also show the multirotor provides the accurate results compared to fixed wing platform. The outcome could be used for specific applications such as urban expansion changes and land cover change detection.

Keywords: *Unmanned; Footprint; Assessment; Area; Length*

1. Introduction

The roles of building footprints from imagery or Digital Surface Model (DSM) data include three-dimensional (3D) building model generation, map updating, urban planning and reconstruction and infrastructure development. The process of data collection to extract building footprints is laborious and time-consuming. The extraction of building data from remotely sensed data is hard due to the character of city environments [4], [6], [9]. Thus, automatic techniques are needed in order to efficiently extract building footprints from large urban areas that contain a lot of buildings. Many automatic techniques have been created within the last few years using different data resources. There are processes done using spectral reflectance values on aerial and high-resolution satellite imagery, however, those techniques frequently encounter problems due to imaging radiometry of optical sensors when similar spectral reflectance of the ground occurs [3]. Building roofs are constructed from different materials with distinct colourations that prompt similar spectral reflectance of building roofs with other items on the ground. Thus, it leads to incorrect extraction of buildings [2], [8]. The layer of buildings is a key reference dataset. It is important to have an up-to-date, current and complete building information. Government agencies and the private sectors are spending millions each year to collect building footprint information from aerial photography [7]. The UAVs provide a high-resolution data that can be adjusted according to the desired overlap and sidelap of image and their operations can be affected by the wind [1], [10]. Different platforms were used in this study, namely, fixed-wing UAV and multi-rotor UAV, and the results of both UAVs were analysed.

Extraction of building footprint depends on image resolution. Resolution is defined as the linear dimension of the cell times two (diagonal). There is no scale for a grid map, only a resolution. Graphic representation on a computer screen or printer with one or more pixels (picture elements) includes the smallest areas of the display device that can receive a separate graphic treatment (colour or intensity) [5], [11], [13]. A graphic scale depends on the actual size of the image on the output device compared to the feature being represented. Therefore, ground sampling distance is the relation between the measurement on the image and on the ground. A stereoscopic aerial photograph could provide accurate planimetric coordinates of orthophoto and also height coordinate based on a digital terrain model [12]. This study analysed different algorithms in image matching to perform relative orientation in order to extract building footprints from the selected study area.

2. Data and Materials

Methodology is the most important part of a study. The methodology for this research is divided into four phases. Phase 1 is data preparation which includes camera calibration, UAV calibrations and selection of study area. Phase 2 comprises data collection in the study area including flight planning and acquisition of UAV images. Phase 3 is data processing of all photogrammetric software. This phase also explains the use of three different image matching algorithms to perform relative orientation for stereo model. Phase 4 covers the analysis of data. The overall methodology illustrates the entire process from preliminary study to data processing and finally the results of this study. Phantom 3 Professional was used for image acquisition for multi-rotor UAV and eBee was used for fixed-wing UAV. All acquired images were processed using photogrammetric software. Altizure was used to create the flight planning for capturing image using multi-rotor UAV. The altitude was set at 100 m, while the overlap was 70% and the sidelap was 50%. The reason using these percentages to

overcome the wind effect during the image acquisition to maintain the overlapping images. The overlapping images is very important in photogrammetric image processing to perform image matching for relative orientation. The calculation of distance between strips is described in Equation 1.

$$DS = G - (G \times S) \tag{1}$$

where;
DS = Distance between strips
G = Ground Coverage
S   = Percentage of Side lap

In this study, the calibrated focal length is 3.75mm. Therefore, the total flight lines were four, while the time needed to fly to capture the entire photo was 9.34 minutes. The area was 572 m × 195 m and the speed of the UAV was 5m/s. Figure 1 shows the flight planning created using Altizure.
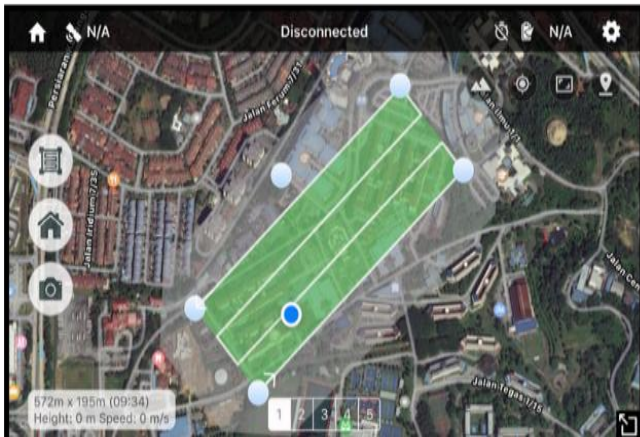

Fig. 1: Flight Planning

Once data collection is completed, the next stage is data processing, where all acquired images will be processed. All images obtained during data acquisition will be imported to photogrammetric software. Then, all images will be automatically set in their position because the images are geotagged with coordinates during image acquisition. The alignment of images is divided into high, medium and low. All results will then be divided into these three categories. The high category involves the calculation of four corners of the digital images plus one coordinate at the centre. The medium category involves the calculation of two corners of the digital images plus one coordinate at the centre. The low category only uses the coordinate at the centre to align the images. Figure 2 illustrates the three methods used in this study to align the images.
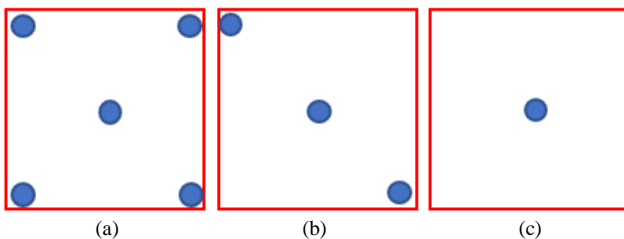

(a)   (b)   (c)
Fig. 2: Image Alignment Methods; a) High, b) Medium, c) Low

After importing all images into the software, they will be self-oriented. The image matching algorithm used in this study consists of three methods, namely, feature-based matching, area-based matching and relational matching. However, epipolar resampling must be performed because visualisation of the stereoscopic model whose images have been acquired with appreciably different angles can be tedious for operators. This is so because the two images have two different scales and orientations. The performance of the image matching technique is also degraded by this type of

image. The epipolar resampling is solved when the point on the left image and conjugate point on the right image from two perspective centres have epipolar axis and focus on one point on the ground where all points must be located in the same plane. Once the condition has been fulfilled, image matching can be performed. The algorithm for the three image matching methods is described in Equations 2-4.

Cross correlation for area based matching

$$\rho = \frac{\sum((g_{TA} - \overline{g}_{TA}) \cdot (g_{SA} - \overline{g}_{SA}))}{\sqrt{\sum((g_{TA} - \overline{g}_{TA})^2) \cdot \sum((g_{SA} - \overline{g}_{SA})^2)}} \tag{2}$$

where;
g = grey value (density) in a position
g = arithmetic mean of the grey values (densities) in that window.
TA = Target Area, the template.
SA = Search Area, the matching window

Moravec operator for feature based matching

$$M_{(r,c)} = \sum_{i,j}\left((g_{(r,c)} - g_{(i,j)})^2\right) \tag{3}$$

Relational matching is based on relationship between objects (distances, angles, collinearity)

$$d = \sqrt{(\partial x^2 + \partial y^2)} \tag{4}$$

where;
d = distance
∂x = difference in x
∂y = difference in y

After the images have been imported, they will be aligned. Then, Place Markers for Ground Control Points (GCPs) will be marked in the images. Afterwards, three different image matching methods will be applied to build dense cloud, followed by triangular irregular network to create a surface on each of the three points, and generate Digital Terrain Model (DTM) and orthophoto. There are six GCPs to be marked in the images. The GCPs are established using Rapid Static method and the observation time is 20 minutes. As for the Digital Surface Model (DSM), DTM and orthophoto can be obtained using the photogrammetric software, then, the results will be processed using ArcGIS to build extraction. From the generated DSM and DTM, the parameters that will be considered to distinguish a building from other features are height and area. The range of height used for extraction is between 30 to 50m. Smaller features that may be extracted as buildings can be resolved by filtering the extracted features according to the area. The range of area used for extraction is between 1200 to 2000m². The final step for building extraction is the simplification of the polygons extracted to eliminate irregular shaped features.

3. Results and Analysis

Photogrammetric software was used to process the images and three different image matching algorithms were used, as mentioned in the methodology section. Each type of accuracy was used in this study to see the effects on the results. DTM, DSM and orthophoto were the results obtained each time the UAV images were processed by the photogrammetric software. Figure 3 illustrates the examples of orthophoto, DSM and DTM in the study area.
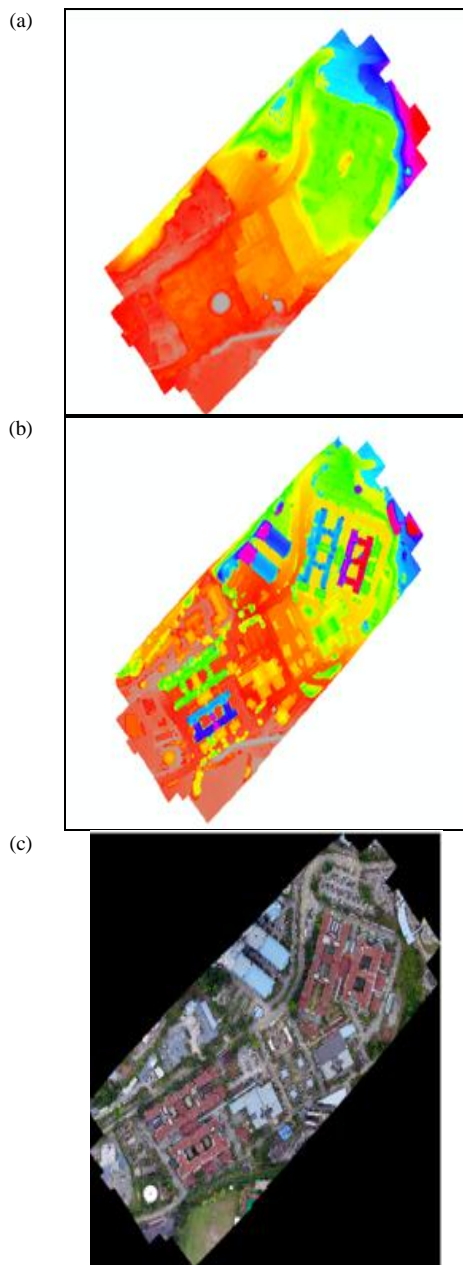
(a)

(b)

(c)

Fig. 3: Results; (a) DTM, (b) DSM, (c) Orthophoto

DTM, DSM and orthophoto were processed using a third party software to extract the building footprints. The building footprints were extracted based on the outcome of subtraction between DSM and DTM, filtration of the height range and area of the desired building and lastly simplification of building polygons. Analysis on the area and length can be assessed after the extraction process is completed, and the area and length can be measured using tools in the third party software. Figure 4 illustrates the examples of extraction of building footprints.
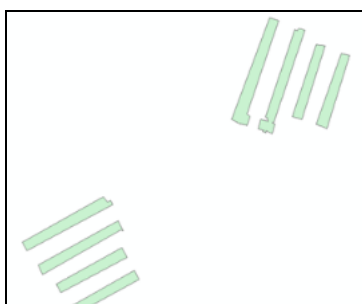

Fig. 4: Some Example on Building Footprints

Figure 5a describes the root-mean-square-error (RMSE) of the measurement of the area in high alignment category using three different image matching methods for multi-rotor and fixed-wing UAVs. The differences in the RMSE results between multi-rotor and fixed-wing UAVs for area-based matching method, feature-based method and relational matching are 4.443m^2, 11.149m^2 and 14.303m^2, respectively. The type of UAV and the three different image matching methods influence the measurements of area. Figure 5b describes the RMSE of the measurement of the area in medium alignment category using three different image matching methods for multi-rotor and fixed-wing UAVs. The differences in the RMSE results between multi-rotor and fixed-wing UAVs for area-based matching method, feature-based method and relational matching are 5.375m², 9.671m^2 and 6.334m^2, respectively.
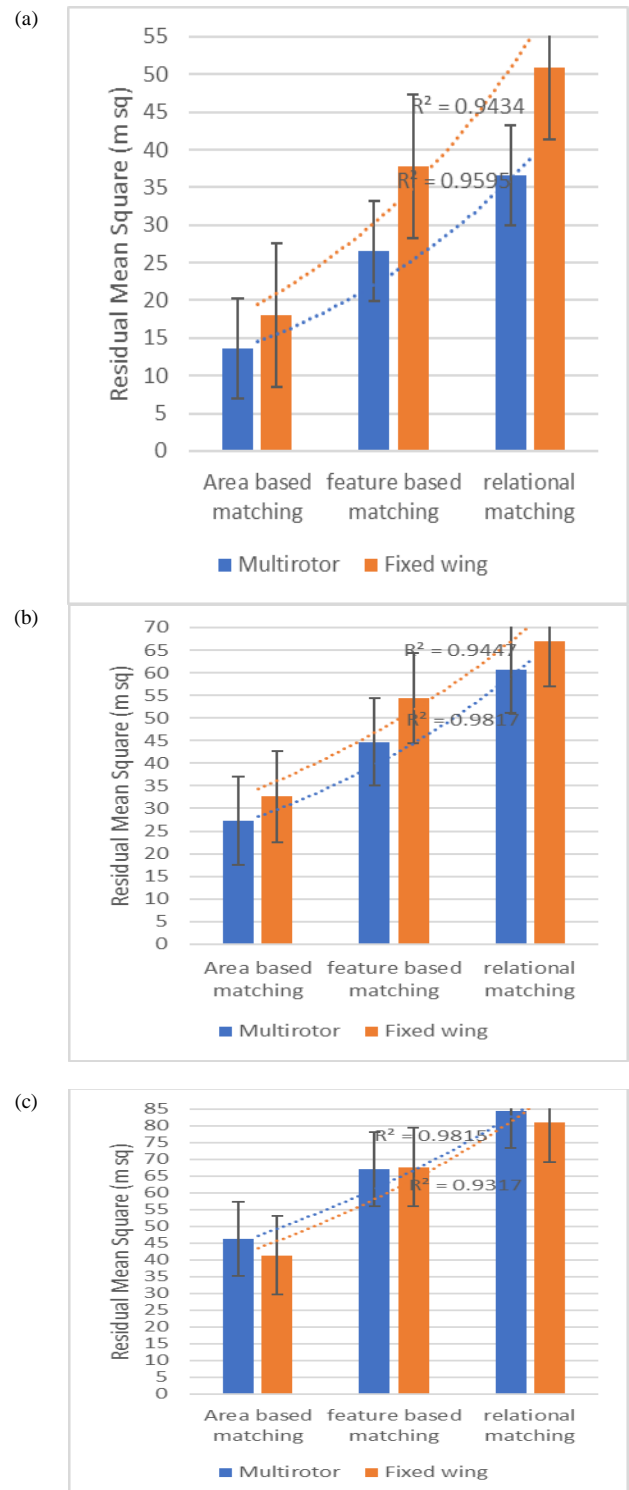
(a)

(b)

(c)

Fig. 5: RMSE of Area; (a) High, (b) Medium, (c) Low

Figure 5c describes the RMSE of the measurement of the area in low alignment category using three different image matching methods for multi-rotor and fixed-wing UAVs. The differences in the RMSE results between multi-rotor and fixed-wing UAVs for area-based matching method, feature-based method and relational matching are $4.785m^2$, $0.644m^2$ and $3.487m^2$, respectively. Based on Figure 5, it can be seen that the low alignment method produced the smallest difference among the three different image matching methods using fixed-wing and multi-rotor UAVs. The high alignment category generated the biggest difference between multi-rotor and fixed-wing UAVs for all three different image matching methods. Figure 6a describes the RMSE of the measurement of length in high alignment category using three different image matching methods for multi-rotor and fixed-wing UAVs. Based on Figure 6a, the differences in RMSE results between multi-rotor and fixed-wing UAVs for area-based matching method, feature-based method and relational matching are 93mm, 2mm and 77cm, respectively.
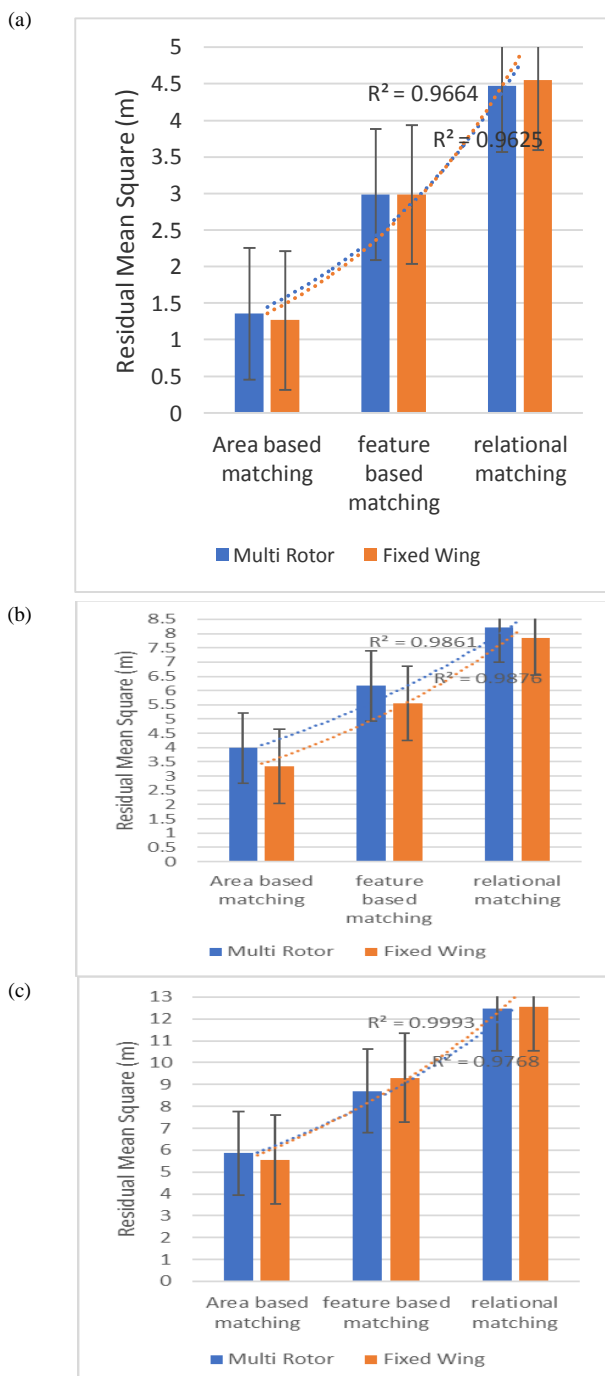
Figure 6b describes the RMSE of the measurement of length in medium alignment category using three different image matching methods for multi-rotor and fixed-wing UAVs. The differences in RMSE results between multi-rotor and fixed-wing UAVs for area-based matching method, feature-based method and relational matching are 0.642m, 0.597m and 0.361m, respectively. Figure 6c describes the RMSE of the measurement of length in low alignment category using three different image matching methods for multi-rotor and fixed-wing UAVs. The differences in RMSE results between multi-rotor and fixed-wing UAVs for area-based matching method, feature-based method and relational matching are 0.285m, 0.623m and 0.087m, respectively. Based on Figure 6, it can be seen that high alignment category generated the smallest RMSE difference among all three image matching methods using multi-rotor and fixed-wing UAVs. This is contrary to the assessment on the area as the low alignment category gave the smallest difference. Besides, the area-based matching showed the lowest accuracy compared to other image matching methods.

4. Conclusion

The extraction of building footprints was successfully done using ArcGIS. The area and length measurements were compared with the actual data using the existing layout plans. It shows the comparison of building footprints by using multi-rotor and fixed-wing UAVs. The effects on the results from each accuracy were successfully analysed. In this study, building extraction was performed using NDSM generation, followed by extraction by height and area, raster to vector conversion and lastly building simplifications. Based on the RMSE results, it can be said that, the assessment on the area provided the smallest difference for low alignment category, while the assessment on length produced the smallest difference for high alignment category. The area-based matching method generated the lowest accuracy compared to feature-based and relational matching methods. Overall, measurements of multi-rotor UAV were much closer to the measurements of the existing layout plans compared to the measurements of fixed-wing UAV.

Acknowledgement

References

[1] Abu Hanipah, A.F.F & Tahar, K.N.: Development of the 3D dome model based on a terrestrial laser scanner. International Journal of Building Pathology and Adaptation, 36: 2, 122-136, 2018.

[2] Asahari, M.N. & Tahar, K.N.: Building Footprint Assessment Based on Onboard Global Positioning System and Ground Control Points. Advanced Science Letters, 23: 5, 3849-3853(5), 2017.

[3] Agius, C., & Brearley, J.: Can Building Footprint Extraction from LiDAR be used Productively in a Topographic Mapping Context? In Future Preparedness: Thematic and Spatial Issues for the Enviroment and Sustainability, 60-73, 2014.

[4] Burdeos, M. D., Makinan-Santillan, M., & Amora, A.: Automated Building Footprints Extraction from DTM and DSM in ArcGIS. MDA Burdeos, 2015.

[5] Dahiya, S., Garg, P.K., & Mahesh, K.J.: Building Extraction from High Resolution Satellite Images. ECHNIA – International Journal of Computing Science and Communication Technologies, VOL.5 NO. 2, Jan. 2013 (ISSN 0974-3375), 829-834.

(a)

(b)

(c)

Fig. 6: RMSE of Length; (a) High, (b) Medium, (c) Low

[6] Davydova, K., Cui, S., & Reinartz, P.: Building Footprint Extraction from Digital Surface Neural Networks. German Aerospace Center (DLR), Remote Sensing Technology Institute (IMF),. Oberpfaffenhofen,Germany., 2016.

[7] Delgado, F.S., Carvalho, J.P., Coelho, T.V.N. & Dos Santos, A.B.: An Optical Fiber Sensor and Its Application in UAVs for Current Measurements. Sensors, 16, 1800, 2016.

[8] Grenzdörfer, G., Guretzki, M. & Friedlander, I.: Photogrammetric image acquisition and image analysis of oblique imagery. The Photogrammetric Record, 23 (124), 372-368, 2008.

[9] Jabari, S., Fathollahi, F., Roshan, A., Zhang, Y.: Improving UAV imaging quality by optical sensor fusion: an initial study. International Journal of Remote Sensing, 38:17, 4931-4953, 2017.

[10] Junaid, A., Lee, Y. & Kim, Y.: Design and implementation of autonomous wireless charging station for rotary-wing UAVs. Aerospace Science and Technology, 2-14, 2015.

[11] Martinez, S., Ortiz, J. & Gil, M. L.: Geometric documentation of historical pavements using automated digital photogrammetry and high-density reconstruction algorithm. Journal of Archaeological Science, 1-11, 2015.

[12] Meena, Y. & Mittal, A.: Blobs & Crack Detection on Plain Ceramic Tile Surface. International Journal of Advanced Research in Computer Science & Software Engineering, 3, 2013.

[13] Tahar, K. N.: Multi Rotor UAV at Different Altitudes for Slope Mapping Studies. The International Archives of the Photogrammetry, Remote Sensing and Spatial Information Sciences, Volume XL-1/W4, 2015, (pp. 9-16). Toronto, Canada, 2015.

[14] Wei, W., Xu, Q. & Wang, L.: GI/Geom/1 queue based on communication model for mesh networks [J]. International Journal of Communication Systems. 27, 11, 2014.